H. C. Nguyen, G. R. MacCartney, Jr., T. A. Thomas, T. S Rappaport, B. Vejlgaard, and P. Mogensen, " Evaluation of Empirical Ray-Tracing Model for an Urban Outdoor Scenario at 73 GHz E-Band," in *Vehicular Technology Conference (VTC Fall), 2014 IEEE 80th*, Sept 14 - 17, 2014.

Evaluation of Empirical Ray-Tracing Model for an Urban Outdoor Scenario at 73 GHz E-Band

Huan Cong Nguyen*, George R. MacCartney Jr.†, Timothy Thomas‡,
Theodore S. Rappaport†, Benny Vejlgaard‡ and Preben Mogensen*
*Department of Electronic Systems, Aalborg University, Denmark, Email: {hcn|pm}@es.aau.dk
‡Nokia Solutions and Networks, Email: {timothy.thomas|benny.vejlgaard|preben.mogensen}@nsn.com
†New York University, Email: {gmac|tsr}@nyu.edu

Abstract

In the summer of 2013, a wideband propagation measurement campaign using rotating directional antennas at 73 GHz was conducted at the New York University (NYU) campus, in order to collect extensive field measurements for use in a millimeter wave (mmWave) E-band statistical channel model. While the measurement campaign provided over 50 Gigabytes of wideband power delay profiles and angular responses [1], [2], the time and labor intensive measurements were based on only 5 transmitter (Tx) locations and 27 receiver (Rx) locations, making up a total of 74 Tx-Rx link combinations. To help generalize the measurements for immediate model development and eventual site planning, this paper presents an empirical ray-tracing model, with the goal of finding a suitable approach such that ray-tracing (RT) can fill in the gaps of the measurements. Here, we use the measured data to investigate the prediction capability of an empirical RT model, in which the 3D model of New York City (including the building structures and interaction losses) are greatly simplified. The comparison between the measured and predicted results show good accuracy is obtained when a simplified RT model is used, suggesting that fast and simple ray tracers will be able to correctly predict the propagation characteristics at mmWave bands.

I. Introduction

The rapid increase of wireless Internet usage via smartphones and tablets has led to an exponential demand for data capacity and download speeds on cellular networks. There are many ways to cope with the increased data traffic demand, but promising approaches fall into three basic options: 1) enhance the spectral efficiency (air interface) of the communication link, 2) implement significant network densification through the deployment of small cells, and 3) increase the allocated spectrum for the mobile network. Today, cellular network deployments are typically done at frequencies below 6 GHz, and in most cases below 3.5 GHz. Given the limited spectrum available below 6 GHz, and the growing demand for data services, this spectrum alone cannot keep up for predicted demand into the next decade [3]. On the other hand, a vast amount of spectrum above 6 GHz remains underutilized, particularly in the millimeter wave (mmWave) bands between 30-300 GHz. Here, there are tens of gigahertz of unoccupied spectrum to support mobile broadband systems. In addition, the very short wavelength of the mmWave bands allows manufacturers to put many more antennas into the same physical size, which facilitates the usage of Multiple Input Multiple Output (MIMO) technology to achieve higher gain and/or better spatial multiplexing [4]. Such advantages have brought significant interest in mmWave communication, both from industry and academia, with a growing belief that mmWave bands will play an important role in beyond 4G and 5G cellular systems [5].

Before mmWave communication systems can be designed and actualized, it is essential to understand how mmWave signals propagate in all potential use-case scenarios. One such case is the outdoor urban scenario, where dense and tall building structures often obstruct the line-of-sight (LOS) condition, causing severe shadowing, which is particularly harmful for mmWave communications. In order to realistically assess mmWave propagation in urban environments, extensive wide-band channel measurement campaigns have been made in outdoor urban environments in Austin, Texas and New York City [3], [6]. In particular, a campaign focused on the 73 GHz frequency band, part of the 71-76 GHz, 81-86 GHz and 92-95 GHz spectrum available for indoor and outdoor wireless communications, was performed in the summer of 2013 [1]. The measurements were conducted at 5 Tx and 27 Rx locations around NYU's downtown Manhattan campus, located in a dense urban neighborhood of New York City. In total, 74 Tx-Rx link combinations was measured. The surrounding environment included large buildings, foliage, and pedestrian and vehicular traffic, which are very common aspects in dense urban layouts. It was necessary to perform measurements six days a week and approximately 10 hours per day throughout an entire summer in order to obtain enough results to accurately model the mmWave E-band channel [1], [2]. Over 50 Gigabytes of raw data was obtained, as wideband power delay profiles for exhaustively searched angles of arrival and departure were conducted. Due to the extreme amount of time and labor required to obtain measurements from many spatial directions at many locations, it is important to investigate ray-tracing (RT) models that can accurately corroborate the field measurements while predicting propagation at mmWave bands. In particular, the limited number of Tx and Rx sites gives relatively few measurement points from

which to develop a statistical channel model. Additionally, the difficulty in scanning many Tx and Rx angles in both azimuth and elevation leave gaps in the measurements, particularly in the elevation dimension from the Tx, which is critical to channel modeling, given the fact future mmWave devices will likely use 2D arrays at mmWave [3]. The RT tool enables a natural way to fill in the measurement gaps in the elevation dimension until more measurements are available, and allows researchers to specifically answer questions about the distance-dependence of elevation parameters. One such elevation parameter is elevation spread which is defined as the root mean square (rms) angle spread relative to the mean elevation angle and a second such parameter is the elevation angle bias which is the mean elevation angle relative to the LOS angle. In fact, same RT predictions used in this paper were used in [7] to develop a 3GPP-like mmWave channel model that includes the modeling of the distance-dependence of the elevation parameters.

Various form of ray tracing have been shown to work well in micro cellular environments in the 1-5 GHz range [8], [9], [10], [11] but mmWave is a new frontier that presently is not well-addressed by commercial ray tracers. At lower frequency bands, the diffraction is a fundamental propagation mechanism [12], but will be much less dominant at mmWave. The scattering and reflection, as well as LOS are the critical components at mmWave. In this paper an empirical RT model is evaluated at mmWave bands using the knowledge gathered from the measurement campaign, although ongoing work is continuing to validate the extensive temporal multipath clusters. The RT model is chosen because it has important simplifications that allow prediction of large outdoor areas within reasonable computation times. The details of the model are given in the Appendix. The remainder of the paper is organized as follows: In Section II we discuss the measurement setup and procedure. The measurement results are presented in Section III in comparison with RT prediction, and finally the conclusions are drawn in Section IV.

II. Measurement Campaign & Procedure

Test locations for the 73 GHz propagation measurement campaign were selected based on previous 28 GHz wideband directional measurements around NYU's campus during the summer of 2012 [3], [13], [14]. Overall, five distinct transmitter (Tx) and 27 distinct receiver (Rx) locations were used for measurements (see Fig. 1). All Tx antenna locations were at heights of 7 m relative to ground level, except for the TX-KAU, which was located on the 5^{th} story balcony of the Kaufman Building at a height of 17 m above ground. Rx locations were tested with antennas at two different antenna heights depending on the scenario. For backhaul-to-backhaul (BH-BH) scenarios the Rx antenna was elevated via a pneumatic mast to a height of 4.06 m relative to ground, and was then lowered to 2 m relative to ground for base-station-to-mobile (BS-MS) measurements.

In order to measure a wireless channel, specific equipment and technologies are needed for accurate and high resolution recordings. The 73 GHz campaign employed a sliding correlator channel sounder system that was first presented by D. Cox in [15]. The channel sounder transmitted a 400 Mcps baseband pseudorandom 11th order m-sequence that was BPSK modulated onto the Radio Frequency (RF) frequency of 73.5 GHz with a first null-to-null bandwidth of 800 MHz. Due to the shorter wavelengths and less favorable propagation characteristics of mmWaves compared to traditional bands below 6 GHz, rotatable high-gain directional antennas were used for measurements. Both the Tx and Rx used steerable 27 dBi antennas with 7^o half-power beamwidths. The transmit power at the Tx was 14.6 dBm resulting in an equivalent isotropically radiated power (EIRP) of 41.6 dB. More specifications regarding the channel sounder hardware and further results of 73 GHz wideband measurements can be found in [1], [2].

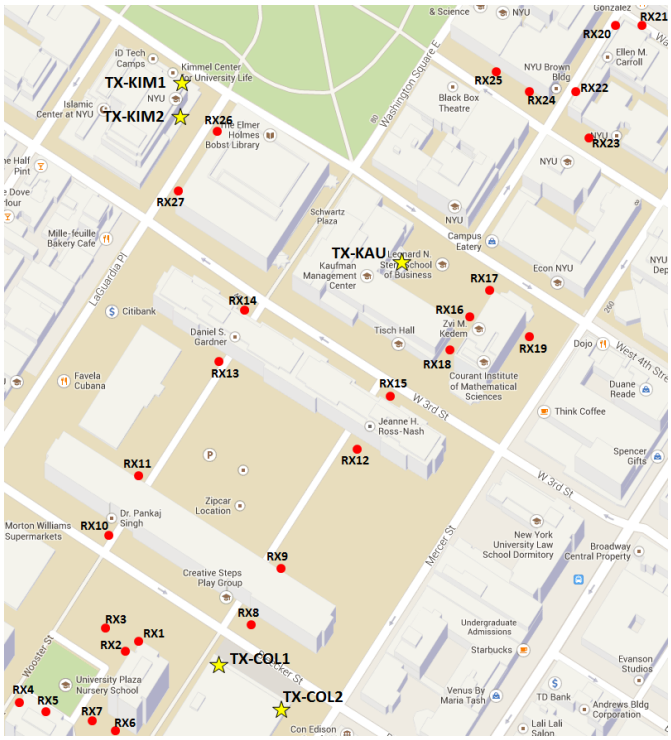

Fig. 1. Map layout of the 73 GHz measurement campaign in the summer of 2013 around NYU's Manhattan campus. Yellow stars correspond to Tx locations and red dots correspond to Rx locations.

The measurement procedure involved steering the Tx and Rx antennas mechanically in the azimuth and elevation plane using FLIR gimbals with 1/3 a degree of accuracy, which meant to mimic an omni-directional antenna. For each Tx-Rx pair, both antennas were exhaustively swept in the elevation and azimuth planes to find the combination resulting in the strongest received power at the Rx side. Such a combination is referred to as *the best measured pointing angle combination*, which indicates that the Tx and Rx antennas are aligned along the dominant propagation path. Once the best angle combination is determined, the Rx antenna is swept 360^o in the azimuth plane in 10^o increments for a LOS environment and 8^o increments for a non line-of-sight (NLOS) environment.

At each increment in the azimuth plane, a Power Delay Profile (PDP) is recorded at the Rx, thus resulting in up to 45 PDPs for one 360^o sweep for a fixed Tx and Rx elevation pointing angles in a NLOS environment. This first sweep corresponds to one measurement configuration. After the initial Rx sweep, another two Rx sweeps were conducted with the Rx antenna elevation uptilted and downtitled by one half-power beamwidth relative to the strongest received Rx antenna elevation. Then the Rx elevation is set back to the strongest elevation while the Tx antenna elevation is uptilted and downtilted by one half-power beamwidth relative to the strongest received Tx antenna elevation for 2 more Rx sweeps. This resulted in five initial measurement configurations. Then, the Rx antenna was fixed in the strongest received azimuth and elevation orientation for one Tx antenna sweep. After the first Tx antenna sweep, the Rx antenna was maneuvered to another azimuth and elevation orientation with strong received power and an additional Tx antenna sweep was conducted. Observations from the Tx antenna sweeps yielded an additional angle of departure to use for five more Rx antenna sweeps that were performed in a similar fashion to the first five. Thus, for one Tx-Rx scenario location combination, up to 12 measurement configurations were conducted, and up to 540 individual PDPs were recorded. In total, 36 base-station-to-mobile and 38 backhaul-to-backhaul Tx-Rx location combinations were tested during the measurement campaign. However, 6 combinations for both BH-BH and BS-MS resulted in outages where no signal was recordable above the system's noise floor. Over the entire stretch of the campaign, thousands of PDPs were recorded and statistics of those PDPs were aggregated into a database for further analysis that is performed in the following RT analysis.

III. Measurement vs Ray-Tracing Results

A 3D model of the NYU campus, where the measurement campaign took place, was created from Open Street Map. The environmental model considered a 600 m x 300 m area and includes only building structures in the area, without foliage and other obstacles in the street. Each building is modeled by a polygon representing its ground area and a corresponding height. We observe that there are a few discrepancies in building shapes and heights between Open Street Map and Google's satellite imagery, but we purposely did not correct our database so we could learn the effect of the 3D model inaccuracy. We further greatly simplified the model by assuming all building materials and ground surfaces have constant and identical material properties for RT predictions, resulting in reflection loss coefficients that are easily applied. The reflection coefficients for reflections were based on commonly-used parameters for lower frequency bands, which are $L_R^{max} = 7$ dB, $L_I^{max} = 8$ dB, $L_I^{min} = 15$ dB and $L_D = 5$ dB, and their meanings are explained in the Appendix. We found that these reflection and diffraction values provided very comparable results to the measured data as given in [1], [2].

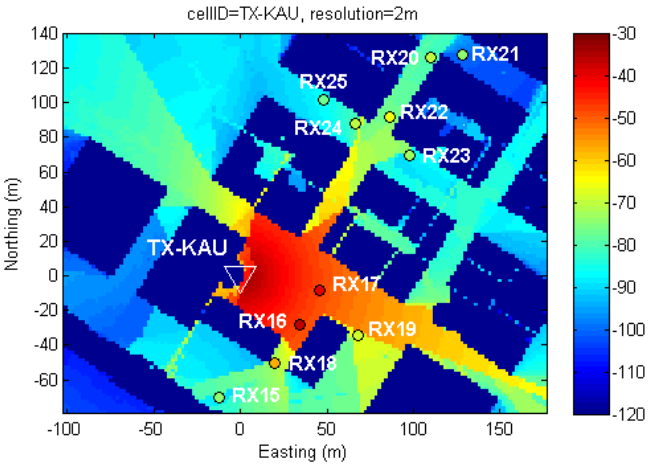

Fig. 2. Predicted received power (in dBm) vs measurement.

A. Large-Scale Path Loss

Fig. 2 shows the actual measured received powers in New York City for all available Tx-Rx pairs from the exemplary transmitter location TX-KAU (shown as the triangle) as overlaid on the power predicted by RT. Note that all measurement values presented in this section are taken from the best measured pointing angle combination [1], [2], unless otherwise stated. For a fair comparison, the same assumption is applied for RT data, where Tx and Rx antennas in the ray tracer are made to each have 27 dBi gains and are tuned to the dominant propagation path similar to the field measurements. In general, the estimated powers are in agreement with the measured ones, with a rms error around 12 dB for both BS-MS and BH-BH scenarios. This error is not large when considering the facts that the measurements are made over a 70 dB dynamic range with the open source 3D model inaccuracies (e.g. a LOS condition is observed in prediction, while it is actually NLOS due to foliage) and the prediction inaccuracies due to the gross simplifications of building material reflection coefficients and interaction loss, without any consideration for scattering.

A critical aspect to be assessed in mmWave communications is the large scale path loss model, which indicates how the signal degrades with distance. In this paper we adopt the close-in free space reference path loss (also referred to as the log-distance law) model, where the large-scale path loss over the distance d is given by the path loss at a reference distance d_0 plus an additional path loss. This is actually a better, more physically accurate model for propagation than common models used in 3GPP (See [1], [2], [5]). The large scale path loss model is as follows:

$$\mathrm{PL}(d) = \mathrm{PL}(d_0) + 10n\log_{10}\left(\frac{d}{d_0}\right) + \xi \qquad (1)$$

where $\mathrm{PL}(d)$ is the average path loss in dB for a specific Tx-Rx separation distance of d in meters, d_0 is the close-in free space reference distance, n is the path loss exponent characterizing how fast the path loss increases with distance, and $\xi \sim \mathcal{N}(0, \sigma^2)$ is the variation due to shadow fading. In our analysis, the path loss is considered as the difference

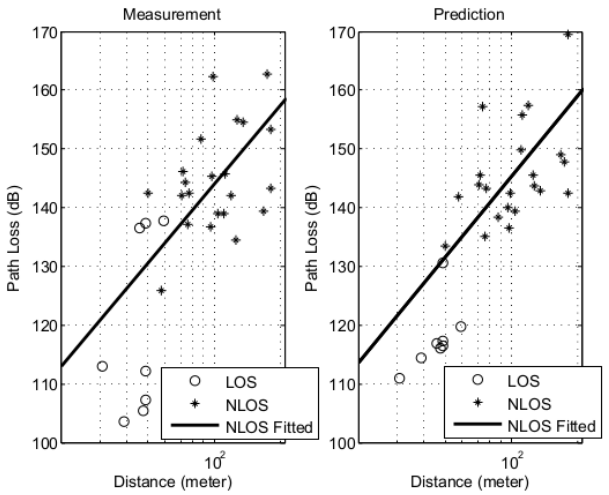

Fig. 3. Measured vs estimated path loss in base-station-to-mobile scenario for all measured RX locations. The comparisons in path loss exponent are made for the case of the ray tracer using identical locations and antenna patterns, and using the best pointing angles for single beam antennas at each location, just as was measured and presented in [1], [2]. Here, we combine all TX heights as multiple measurements for a given RX location, and pick the best pointing angles for a fair comparison.

between received power and transmitted power, and requires the subtraction of the maximum Tx and Rx antenna gains to remove antenna effects. Both measurement and ray-tracing path loss used 4 m close-in reference distance, as this is in the far-field region of both horn antennas [1]. Fig. 3 indicates the measured and predicted path loss for all available Tx-Rx pairs in the BS-MS scenario in New York City, where we compare the measured data with the predicted ray-traced data on the basis of different Rx heights (e.g. 2 m vs. 4.06 m). The solid line is the path loss slope and is estimated from the measurements data points in the NLOS condition. The shadow fading standard deviation is estimated from the rms error between the true values and the path loss slope. The resulting path loss exponent and standard deviation of the shadow fading component (for the best pointing angle combination at each location) are given in Table I. Note that these values are slightly different from the NLOS best single beam path loss exponent provided in [1], due to the fact that we do not separate the path loss into two different Tx height categories in this paper. We observe that the predicted values are very close the measured values, and the path loss exponent and the shadow fading standard deviation at 73 GHz are not much worse than the NLOS values seen at frequency bands below 6 GHz [16]. And in [2] we find that 28 and 73 GHz channels are surprisingly similar, where 73 GHz are not much more lossy. Although the Rx antennas are placed higher in BH-BH scenario, we do not observe any significant difference in path loss between BS-MS and BH-BH scenario, similar to the measurements reported in [1], [2].

B. Channel dispersion

In this section we consider the mmWave channel dispersion in both time and angular domain. The most common measure to characterize the time dispersion of a multipath channel is

TABLE I
PATH LOSS MODEL PARAMETERS

Scenario	n	σ
Base-station-to-mobile (measured)	4.5	8.60 dB
Base-station-to-mobile (predicted)	4.6	7.97 dB
Backhaul-to-backhaul (measured)	4.6	8.54 dB
Backhaul-to-backhaul (predicted)	4.6	9.68 dB

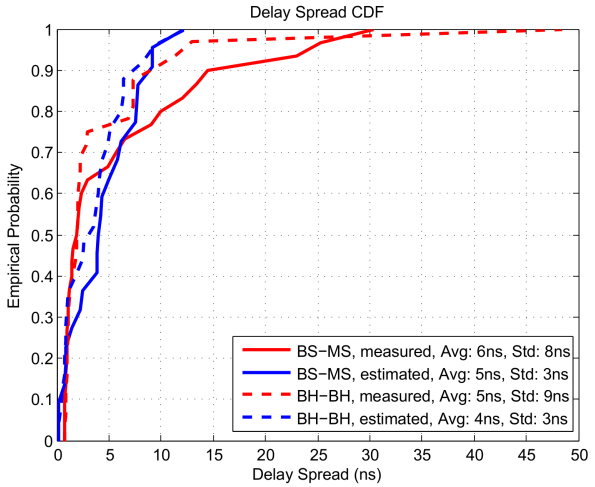

Fig. 4. Measured vs estimated delay spread of the mmWave channel. *Avg* indicates average value, and *Std* means standard deviation.

the rms delay spread, which is defined as the square root of the second central moment of the PDP. Fig. 4 shows the cumulative distribution function (CDF) of the measured and estimated delay spread for all available Tx-Rx locations. It shows that the RT predicts shorter time dispersion of the channel than the measurements, most likely due to the fact that scattering in the channel is not considered by the ray tracer. Also, the number of rays considered in our RT simulation is limited to 20 for the sake of computational complexity. We again note little difference between the BS-MS and BH-BH channels, as reported in [1], [2].

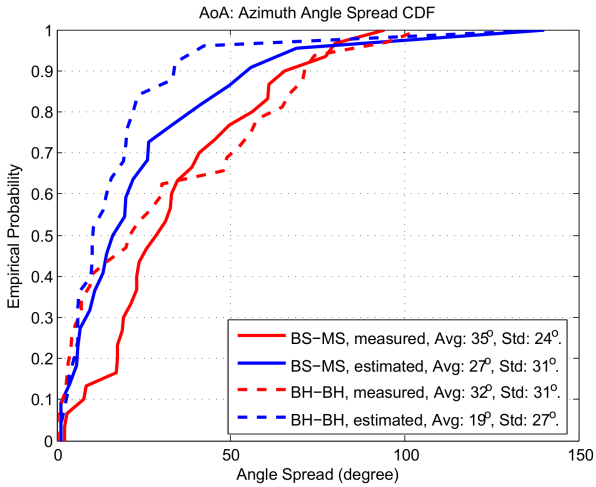

Fig. 5. Measured vs estimated AoA azimuth angle spread.

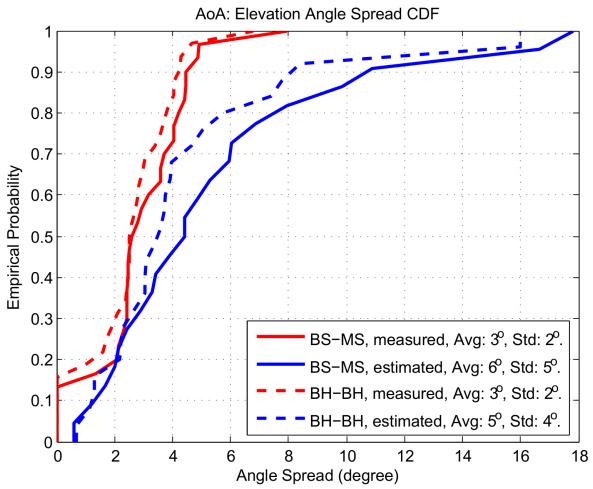

Fig. 6. Measured vs estimated AoA elevation angle spread.

The angular dispersion of the mmWave channel is measured by the elevation and azimuth angle spreads. There are several methods of calculating the angle spread, and in this paper we adopt the guideline in [17]. The Tx antenna is fixed at the best bearing angle, and the angle spread is calculated based on the power and angular information at the Rx side for all available Rx locations. Fig. 5 and 6 shows the CDF of the azimuth and elevation angle spreads, respectively. The predicted azimuth angle spread is generally less than the measurement, whereas the elevation angle spread is greater. The latter is most likely because the measurement campaign does not cover all elevation angles, which resulted in the elevation angle spread being limited to only the few different pointing angles used in the field. Both predicted azimuth and elevation spreads indicates the presence of rich multipath clusters in mmWave propagation, which confirms the finding in [2], [3], [5] that mmWave signals will propagate via several NLOS paths rather than a small number of LOS links.

IV. Conclusions

In this paper, the mmWave propagation characteristics are studied via an extensive measurement campaign and a RT exercise. The study focuses on an urban scenario at the 73 GHz band, for both base-station-to-mobile and backhaul-to-backhaul link. The measurements indicate that mmWave signal can be received at up to 200 m in NLOS conditions with the use of high directivity antennas. The RT model, even though simplified and affected by the inaccuracy of the 3D model, is shown to be able to correctly predict the mmWave propagation in the urban environment. No significant difference is observed for base-station-to-mobile and backhaul-to-backhaul links. The inclusion of scattering will further improve the ray tracing approach.

Appendix
Empirical Ray-Tracing Model

The RT model under evaluation is provided by a commercial network planning tool [18]. It is different from standard

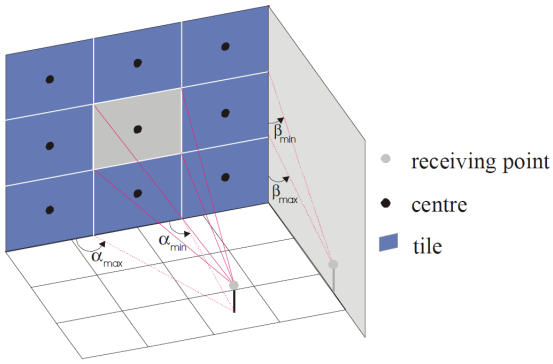

Fig. 7. Tiles of a wall and visibility relation [19].

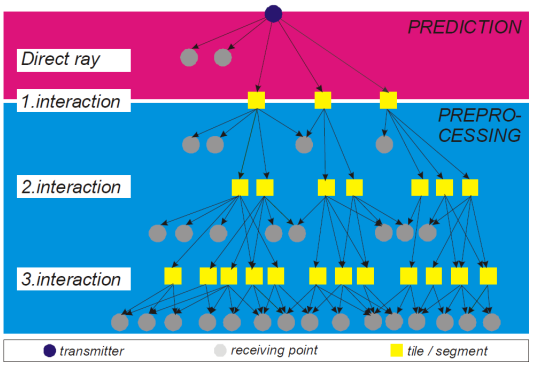

Fig. 8. Tree representing the visibility relations [19].

ray-tracing (or ray-launching) in two aspects, namely the *database preprocessing* and *empirical interaction loss*, both aiming at reducing the computational complexity and time. The database preprocessing refers to the process of dividing all building walls into tiles (for reflections and penetrations), and building edges into horizontal and vertical segments (for diffractions) [19]. In addition, the prediction plane is also divided into a grid of receiving points (see Fig. 7). All elements, i.e. tiles, segments and receiving points, are represented by their centers, which leads to the discretization of the problem of path finding. Once this step is completed, the RT algorithm exhaustively searches for visibility relations between the elements (which indicates potential rays), and creates a tree structure to represent its findings. Each branch of the tree illustrated in Fig. 8 represents a visibility relation between two different elements, and the distances as well as the incident angles between them are determined and stored. Given that the location of elements are fixed in the database, the visibility relations between elements are independent of the transmitter location. Therefore only the relation in the first layer, i.e. between the transmitter and the first element, need to be computed at prediction time. The data preprocessing helps to reduce the RT problem into a search in a finite tree structure, which leads to a significant saving of computational time.

For computation of the path loss at each ray, not only the free space path loss has to be considered but also the loss due to the reflections, diffractions, and transmissions. The standard

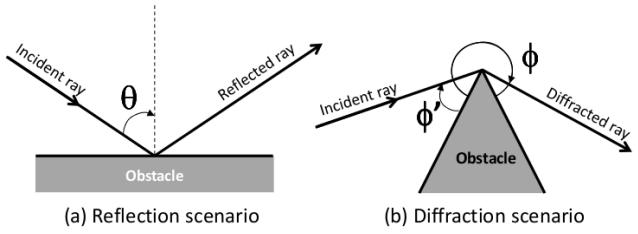

Fig. 9. Definition of angles in reflection and diffraction scenarios

RT model often uses the Fresnel Equation for determination of the reflection and transmission loss, and the uniform diffraction theory (UTD) for calculating the diffraction loss. The empirical RT model proposed a different approach to calculate such losses to further reduce the computation time. The reflection loss in the empirical model depends on the angle of incidence Θ (with respect to the perpendicular line of the wall) and the maximum reflection loss L_R^{max} defined for each material. Eq. (2) indicates that the reflection loss linearly decreases as the angle of incidence increases:

$$L_R = L_R^{max} - \frac{0.5 L_R^{max} \Theta}{90^o} \tag{2}$$

On the other hand, the empirical diffraction model computes the total diffraction loss in a two-step approach based on the three parameters: minimum incident loss of incident ray L_I^{min}, maximum loss of incident ray L_I^{max} and the diffraction loss of diffracted ray L_D [20]. In the first step the loss depending on the incident angle Φ' is determined using Eq. (3). And then the total diffraction loss L_T is calculated as in Eq. (4). It increases as the interaction angle $\Delta_\Phi = \Phi - \Phi'$ increases, where Φ is the diffracted angle. The interaction angle indicates how much the ray has changed its angle due to diffraction phenomenon. In special cases, where the interaction angle is 180^o, the diffraction loss is fixed to 6 dB as the incident wave propagates straight forward while half of the space is shadowed by the given obstacle. Therefore the range of possible total diffraction losses is given by $[6; L_I^{max} + L_D]$ dB.

$$L_I = \begin{cases} L_I^{max} - \frac{(L_I^{max} - L_I^{min})\Phi'}{90^o} & \Phi' < 90^o \\ L_I^{min} & \Phi' \geq 90^o \end{cases} \tag{3}$$

$$L_T = \begin{cases} L_C & \Delta_\Phi \leq 90^o \\ L_C - \frac{(L_C - 6)(\Delta_\Phi - 90^o)}{90^o} & 90^o < \Delta_\Phi \leq 180^o \\ L_C - \frac{(L_C - 6)(270^o - \Delta_\Phi)}{90^o} & 180^o < \Delta_\Phi \leq 270^o \\ L_C & 270^o < \Delta_\Phi \end{cases} \tag{4}$$

where $L_C = L_I + L_D$.

REFERENCES

[1] G. R. MacCartney Jr. and T. S. Rappaport, "73 GHz millimeter wave propagation for outdoor urban mobile and backhaul communications in New York City," in *Communications (ICC), 2014 IEEE International Conference on*, June 2014.

[2] S. Sun and T. S. Rappaport, "Millimeter Wave Multi-beam Antenna Combining for 5G Cellular Link Improvement in New York City." IEEE Intl. Conference on Communications (ICC), June 2014, Sydney, Australia., 2014.

[3] T. S. Rappaport, S. Sun, R. Mayzus, H. Zhao, Y. Azar, K. Wang, G. Wong, J. Schulz, M. Samimi, and F. Gutierrez, "Millimeter Wave Mobile Communications for 5G Cellular: It Will Work!" *Access, IEEE*, vol. 1, pp. 335–349, May 2013.

[4] T. S. Rappaport, J. Murdock, and F. Gutierrez, "State of the Art in 60-GHz Integrated Circuits and Systems for Wireless Communications," *Proceedings of the IEEE*, vol. 99, no. 8, pp. 1390–1436, Aug 2011.

[5] S. Rangan, T. S. Rappaport, and E. Erkip, "Millimeter-Wave Cellular Wireless Networks: Potentials and Challenges," *Proceedings of the IEEE*, vol. 102, no. 3, pp. 366–385, March 2014.

[6] T. S. Rappaport, F. Gutierrez, E. Ben-Dor, J. Murdock, Y. Qiao, and J. Tamir, "Broadband Millimeter-Wave Propagation Measurements and Models Using Adaptive-Beam Antennas for Outdoor Urban Cellular Communications," *Antennas and Propagation, IEEE Transactions on*, vol. 61, no. 4, pp. 1850–1859, April 2013.

[7] T. Thomas, H. C. Nguyen, G. MacCartney, and T. S. Rappaport, "3D mmWave Channel Model Proposal." Submitted to IEEE VTC Fall 2014, 2014.

[8] T. Tran and T. S. Rappaport, "Site specific propagation prediction models for PCS design and installation," in *Military Communications Conference, 1992. MILCOM '92, Conference Record. Communications - Fusing Command, Control and Intelligence., IEEE*, Oct 1992, pp. 1062–1065 vol.3.

[9] K. Schaubach, I. Davis, N.J., and T. S. Rappaport, "A ray tracing method for predicting path loss and delay spread in microcellular environments," in *Vehicular Technology Conference, 1992, IEEE 42nd*, May 1992, pp. 932–935 vol.2.

[10] R. Skidmore, T. S. Rappaport, and A. Abbott, "Interactive coverage region and system design simulation for wireless communication systems in multifloored indoor environments: SMT Plus," in *Universal Personal Communications, 1996. Record., 1996 5th IEEE International Conference on*, vol. 2, Sep 1996, pp. 646–650 vol.2.

[11] G. Durgin, N. Patwari, and T. S. Rappaport, "An advanced 3D ray launching method for wireless propagation prediction," in *Vehicular Technology Conference, 1997, IEEE 47th*, vol. 2, May 1997, pp. 785–789 vol.2.

[12] T. Russell, C. Bostian, and T. S. Rappaport, "A deterministic approach to predicting microwave diffraction by buildings for microcellular systems," *Antennas and Propagation, IEEE Transactions on*, vol. 41, no. 12, pp. 1640–1649, Dec 1993.

[13] Y. Azar, G. Wong, K. Wang, R. Mayzus, J. Schulz, H. Zhao, F. Gutierrez, D. Hwang, and T. S. Rappaport, "28 GHz propagation measurements for outdoor cellular communications using steerable beam antennas in New York city," in *Communications (ICC), 2013 IEEE International Conference on*, June 2013, pp. 5143–5147.

[14] M. Samimi, K. Wang, Y. Azar, G. Wong, R. Mayzus, H. Zhao, J. Schulz, S. Sun, F. Gutierrez, and T. S. Rappaport, "28 GHz Angle of Arrival and Angle of Departure Analysis for Outdoor Cellular Communications Using Steerable Beam Antennas in New York City," in *Vehicular Technology Conference (VTC Spring), 2013 IEEE 77th*, June 2013, pp. 1–6.

[15] D. Cox, "Delay Doppler characteristics of multipath propagation at 910 MHz in a suburban mobile radio environment," *Antennas and Propagation, IEEE Transactions on*, vol. 20, no. 5, pp. 625–635, Sep 1972.

[16] I. Rodriguez, H. C. Nguyen, N. T. Jørgensen, T. B. Sørensen, J. Elling, M. B. Gentsch, and P. Mogensen, "Path Loss Validation for Urban Micro Cell Scenarios at 3.5 GHz Compared to 1.9 GHz," in *Globecom. IEEE Conference and Exhibition*, 2013.

[17] 3GPP, "Spacial channel model for Multiple Input Multiple Output (MIMO) simulations," 3rd Generation Partnership Project (3GPP), TR 25.996, Sept. 2012. [Online]. Available: http://www.etsi.org/

[18] "AWE Communications - News around AWE Communications," http://www.awe-com.com/News/commercial.html, 2014, [Online; accessed March-2014].

[19] T. Rautiainen, R. Hoppe, and G. Wolfle, "Measurements and 3D Ray Tracing Propagation Predictions of Channel Characteristics in Indoor Environments," in *Personal, Indoor and Mobile Radio Communications, 2007. PIMRC 2007. IEEE 18th International Symposium on*, Sept 2007, pp. 1–5.

[20] "AWE Communications - Empirical Interaction Model," http://www.awe-com.com/, 2013, [Online; accessed Sep-2013].